NUMERICAL STUDY ON HEAT AND MASS TRANSFER BEHAVIOR OF POOL BOILING IN LIBR/H₂O ABSORPTION CHILLER GENERATOR CONSIDERING DIFFERENT TUBE SURFACES

Farshad Panahizadeh[1] ,Mahdi Hamzehei[1][*], Mahmood Farzaneh-Gord[1,2],Alvaro Antonio Ochoa Villa[1,3]

[1]Department of Mechanical Engineering, Ahvaz Branch, Islamic Azad University, Ahvaz, Iran

[2]Department of Mechanical Engineering, Ferdowsi University of Mashhad, Mashhad, Iran

[3]Federal Institute of Technology of Pernambuco, Av. Prof. Luiz Freire, 00, CEP:50740-540, Recife, PE, Brazil

[*]Correspond author email address: mahdi.hamzei@gmail.com;mahdi_hamzei@iauahvaz.ac.ir

Investigating the pool boiling process in the absorption chiller generator by studying the valid parameters may enhance the chiller's coefficient of performance (COP). In the present study, the transient two-dimensional numerical modeling of LiBr/H₂O solution pool boiling in the generator of the absorption chiller was carried out using the two-phase Eulerian-Eulerian approach, extended Rensselaer Polytechnic Institute (RPI) boiling model and renormalization group (RNG) K-ε turbulence model. The numerical model was applied on three types of the bare, notched fin, and low fin tubes to investigate the effect of using fin on the boiling heat transfer rate in the generator of the absorption chiller and comparing it with the bare tube. Moreover, the numerical results were compared with the data obtained from the previous experimental studies to validate numerical modeling. A good agreement was achieved between numerical and experimental results. The results showed the evaporation mechanisms in the microlayer, evaporation in the three-phase (liquid-vapor-solid) contact line, and transient conduction to the superheat layer for constant thermal heat flux and the three surfaces of the copper tube within a specific period from the boiling point of LiBr/H₂O solution. The results also showed that the use of a notched fin-tube and low fin tube increases the non-homogeneous nucleation rate, causes the solution to boil earlier than the bare tube, and reduces the required thermal energy in the generator of an absorption chiller.
Keywords: *Absorption chiller, Generator, Pool boiling, Low fin, Nucleation rate.*

1. Introduction

One of the essential heat exchangers in the absorption chiller is the generator in which the pool boiling of the lithium bromide/water solution occurs [1, 2]. Therefore, improving the heat transfer in this heat exchanger increases energy efficiency and improves the chiller's coefficient of performance (COP) [3, 4]. The boiling phenomena locally have both vapor and liquid phases [5, 6]. From the

mathematical point of view, two phases can be considered as a field with two single-phase regions along with moving boundaries separating the phases. Navier-Stokes nonlinear partial differential equations exist for each phase, and boundary conditions must be applied to the whole field. Considering the interface as the moving boundary is the most crucial issue in solving the boiling flow [7]. Therefore, it is required to consider two-phase models such as the Eulerian-Eulerian model for modeling boiling phenomena, capturing phase's behaviors, and interactions along with the interface between them. Several pieces of research used the Ansys-Fluent CFD package, which relies on finite volume computational methods to study the pool boiling of pure material such as water with a two-phase Eulerian approach with Rensselaer Polytechnic Institute (RPI) boiling model and standard k-Ɛ turbulence model [8].According to the literature review, it has been found that the accuracy of a numerical study of pool boiling phenomena depends on two important parameters: choosing the appropriate two-phase approach and considering the suitable boiling model depending on the geometry and boundary conditions of the problem. Comparing these two critical parameters with experimental data may lead to compatible numerical results. Several studies have been carried out to examine the pool boiling effects in different engineering areas. These studies have focused on the horizontal falling film absorber [9, 10], the boiling heat transfer coefficient in mechanical refrigeration systems [11], the desorption and nucleate boiling in a droplet of $LiBr/H_2O$ solution to check how an increase in the salt concentration of a liquid-layer may lead to a significant decrease in the rate of desorption [12, 13], and the process of stationary evaporation of aqueous solutions [14, 15]. Concerning previous literature, the pool boiling process in the absorption chiller generator might be enhanced by improving the useful parameters, causing an increase in the COP of the chiller. Therefore, in the present study, the numerical modeling of the pool boiling process in the generator of $LiBr/H_2O$ absorption chiller for three types of bare, notched fin and low fin copper tubes have been examined to investigate the effect of using fin on the boiling heat transfer rate and comparing it with the bare tube. Moreover, the Eulerian-Eulerian multiphase approach and extended RPI boiling model have been employed to achieve more accurate results in predicting the boiling behavior of $LiBr/H_2O$ solution in the absorption chiller generator when using different types of tubes.
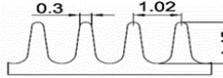
2. Problem Statement

The pool boiling phenomenon is one of the most critical heat transfer methods at high heat fluxes in the absorption chiller generator. Improving this phenomenon may enhance the chiller's COP and reduce the generator's size and cost. Using the extended surfaces is one of the passive methods of pool boiling improvement, which was investigated numerically in the present study. The bare, notched fin, and low fin tubes and their dimensions are presented in Table 1. The low fin tube has an internal diameter of 14.1 mm, an external diameter of 19 mm with 26 fins per inch, and the details illustrated in Table 2. The mentioned dimensions are typical values in the existing absorption chiller. These values were also determined in previous experimental studies [16, 17].

Table 1. Photos and dimensions of sample tubes in the numerical study

Type	Photo	Dimensions	Ref.
Bare		D_i=15 mm D_0=16 mm	[17]
Notched fin		D_i=14.1 mm D_0=16 mm	[16]
Low fin		D_i=14.5mm D_0=19 mm	[18]

Table 2. The detail of fins in the numerical study

Type	Photo	Dimensions	Ref.
Notched fin		Fins per inch: 26, height of fins: 0.37 mm	[16]
Low fin		Fins per inch: 26, height of fins: 1.45 mm	[18]

The dimensions of the model used in the present research are shown in Figure1. The computational dimensions are considered as follows in order to compare the results obtained from the present numerical research with the previous experimental studies by Sim et al. [16, 18].
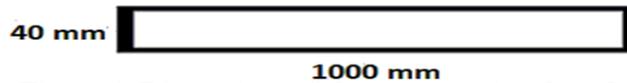
**Figure 1. Dimensions of the computational model**

3. Mathematical Modelling

A two-dimensional model has been constructed in the present study. Two dimensions are considered, one along the length of the tube and the other along the radius. These two dimensions have been determined to illustrate the effect of adding fin to a bare tube on bubble production and growth rate of it in LiBr/H$_2$O solution pool boiling.

3.1. Grid Generation

The geometry of 2D tubes was created in the Ansys DesignModeler, and the computational grid was generated in the ANSYS Meshing software. Node point distribution, smoothness, and elongation of cells affect the mesh quality. The mesh quality should be examined based on the selected mesh. The structured grid has usually been used in numerical studies to increase the grid's quality and reduce the number of computational cells [19]. The accuracy of a numerical solution and its cost regarding required computer hardware and calculation time are dependent on the grid quality. Therefore, in the numerical study, it is necessary to care enough about generating a good quality grid without increasing the number of computational cells. In other words, the resolution parameter is essential in generating the grid for the numerical study of the computational domain. Because of exceeding grid density in one area, data accumulation happens in that area of computational solution, resulting in convergence failure and inaccurate solutions in the computational domain. The computational grid used for this numerical analysis is shown in Figure 2a. Medium size grid applied for tubes, and due to high heat and mass transfer phenomena near the wall with constant heat flux, the boundary layer meshing is applied

3

to capture them well. As shown in Figure 2b, the structured mesh was used to create the computational grid for a bare tube, which includes 29028 quadrilateral cells with an average quality of 0.85 and skewness factor 1. As shown in Figure 2c, the detail of the unstructured grid was used for the notched fin tube with 48235 quadrilateral/trigonal cells with an average quality of 0.87 and skewness 0.9. Figure 2d shows the detail of the unstructured grid was used for the low fin tube with 42235 quadrilateral/trigonal cells with an average quality of 0.85 and skewness 0.9. For notched fin and low fin tube grid generation, several planes were applied in DesignModeler then, considering the multizone method in Ansys meshing, created a higher resolution grid near a fin region. The boundary conditions used for this study are shown in Figure 2e.
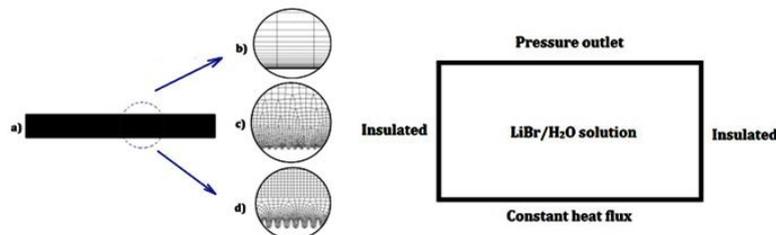
Figure2.a) Computational grid for the numerical study of tubes, b) Details of the computational grid for a bare tube, c) Details of the computational grid for a notched fin, d) Details of the computational grid for a low fin tube, e) Boundary conditions.

3.2. The boundary conditions

The ANSYS Fluent v.19.2, a finite volume-based software, was used in the present study. The boundary conditions are shown in Figure 3. The RNG-based K-Ɛ turbulence model was used because of its ability to analyze boiling problems. Due to the phase change of the vapor-to-liquid in the generator tubes, which transfers the latent heat of the vapor to the surface of the tube, the constant heat flux was considered as the boundary condition for the hot wall ($\dot{q} = \dot{q}_W$). The side walls were determined as insulated ($\dot{q} = -k(dT/dx) = 0$) walls because of low heat transfer in them. The upper boundary condition was also determined as a pressure outlet since the water vaporized from the LiBr/H$_2$O solution was discharged to the condenser. The heated wall roughness was considered constant and equal to 0.5. For the solid-fluid interface of the two phases was considered a non-slip boundary. The saturation temperature of water in atmospheric pressure was considered 373.15 K, and for LiBr/H$_2$O solution, saturation temperature was calculated according to saturation pressure (7 kPa) and solution concentration (50wt.%) equal to 336.9 K.

3.3. Assumptions and theoretical formulation of study

3.3.1 Assumptions

In this study, two-phase Eulerian-Eulerian approximation is used to simulate the phenomenon of pool boiling. LiBr/H$_2$O solution is assumed to be a continuous phase, and water vapor as a dispersed phase, also the properties of the LiBr/H$_2$O solution are considered constant. The side walls are assumed to have no significant force on the bubbles motion.

3.3.2 Governing equations of the modeling

In ANSYS Fluent software, the Eulerian multiphase model solves the continuity and momentum equations for each phase. The energy equation is only determined for the liquid phase, and the vapor phase is assumed to be at the saturation temperature. According to the Eulerian model, the boiling is analyzed based on the wall heat flux partitioning model, which is a subset of the multiphase models. This primary mechanism is also called the Rensselaer Polytechnic Institute (RPI). The wall heat flux divided into three parts, including convective, cooling, and vapored heat fluxes. These elements are calculated using the flow and temperature along with other correlations for nucleation density, bubble diameter during the separation from the surface, and the frequency of the surface separation. This multiphase flow is explained using the following conservation equations [19]. The momentum and energy equations are modeled using the relations listed in the following. When using the RPI model, the vapor temperature is not calculated; however, it is constant at the saturated temperature. For modeling the boiling after the nuclear boiling regime, or its modeling up to the critical heat flux and drying conditions afterward, it is necessary to calculate the vapor temperature. As a result, it is necessary to use other boiling models such as non-equilibrium subcooled boiling (or extended RPI model).

3.3.3 The Extended RPI Model (Non-Equilibrium Boiling Model)

The boiling wall models are compatible with three different wall boundaries: constant wall temperature, definite wall heat flux, and definite wall heat transfer coefficient. Based on the extended RPI model, the wall-to-liquid heat flux is divided into five elements: convective, cooling, and evaporative heat fluxes plus two components of $\dot{q}_V$ and $\dot{q}_G$ that are considered for adding the effect of vapor and gas temperatures [20].

$$\dot{q}_W = (\dot{q}_C + \dot{q}_Q + \dot{q}_E)f(\alpha_l) + (1 - f(\alpha_l))\dot{q}_v + \dot{q}_G \tag{1}$$

$$\dot{q}_C = h_C(T_w - T_l)(1 - A_b) \tag{2}$$

$$\dot{q}_Q = \frac{(T_w - T_l)2k_l}{\sqrt{\pi\lambda_l t}} \tag{3}$$

$$\lambda_l = \frac{k_l}{\rho_l C_{pl}} \tag{4}$$

In the above equations k_l is the thermal conductivity of liquid phase; t is the time of bubble departure; ρ_l, α_l and C_{pl} are the density of liquid phase, liquid volume fraction, and constant heat of liquid phase, respectively.

$$\dot{q}_E = V_d N_w \rho_v h_{fv} f \tag{5}$$

Where V_d is the volume of the bubble, which is calculated by the bubble departure diameter. h_{fv} is the latent heat of evaporation, N_w is the active nucleate site density, and f is the frequency of bubble departure [20, 21].

$$\dot{q}_V = h_V(T_w - T_v) \tag{6}$$

$$\dot{q}_G = h_G(T_w - T_g) \tag{7}$$

$$f(\alpha_l) = 0.5(\frac{\alpha_l}{\alpha_{l,crit}})^{20\alpha_{l,crit}} \tag{8}$$

$$\alpha_{l,crit} = 0.2 \tag{9}$$

Where h_V and h_G are convective heat transfer coefficients of vapor and any other possible gas phase in a system, respectively. T_w, T_v, T_g and $\alpha_{l,crit}$ are wall temperature, vapor temperature, gas

temperature, and constant value, respectively. The superheat temperature difference is calculated as follows.

$$\Delta T_{sup} = T_w - T_{sat} \tag{10}$$

Where T_{sat} is saturation temperature.

In this model, the two most important parameters are the density of the nucleation sites and the diameter of the bubble departing the surface, which are calculated using the following formulas.

$$N_W = C^n (T_w - T_{sat})^n \tag{11}$$

$$d_w = \min\left(0.0014, 0.0006 e^{\frac{-\Delta T_w}{45}}\right) \tag{12}$$

Where n=1.805, C=210, and T_{sat} is saturation temperature.

4. CFD Modeling Assumptions

The assumptions listed in Table 3 have been considered for the modeling process.

Table 3. The assumptions used for this study

Transient-Two Dimensional-Two Phase-Double Precision-Pressure based			
Solver	Eulerian	**Transient formulation**	Second order implicit
Boiling model	Extended RPI [21]	**Time stepping method**	Variable
Boiling Temperature	Saturation temperature according to generator pressure and LiBr/H$_2$O solution concentration	**Minimum time step size(s)**	0.000001
Turbulence model	RNG K-Ɛ	**Maximum time step size(s)**	1
Material	Phase1: LiBr/H$_2$Osolution Phase2: Water vapor	**Number of time steps**	600000
Two phase equations	Drag: Ishii [22]; Lift: Tomiyama [23]; Wall lubrication: Antal-et-al [24]; Turbulent dispersion: Lopez-de-bertodano [25]; Turbulence interaction: Troshko-Hassan [26]; Heat: Ranz-Marshall [27]; Mass: Boiling Bubble departure diameter: Tolubiniski-Kostanchuk [28]; Frequency of bubble departure: Cole [29]; Nucleation site density: Lemmert-Chawla [30]; Surface tension: Constant Interfacial area: Ia-symmetric	**Time of study**	100 second
Pressure-Velocity coupling	Coupled	**Heat flux**	100, 400 kW/m^2
Fluid-solid	Non-slip boundary condition	**Saturation pressure**	7 kPa

5. Thermodynamic properties of the LiBr/H$_2$O solution

The LiBr/H$_2$O solution's thermodynamic properties have been calculated using the engineering equations solver (EES), which are presented in Table 4. A good agreement was achieved between numerical and experimental results to check the accuracy of the obtained properties.

Table 4. The LiBr/H$_2$O properties

Concentration	50	wt.%	Viscosity	0.0038	kg/(m.s)
Density	1533	Kg/m^3	Surface tension	0.0691	N/m
Thermal conductivity	0.4440	W/(m.K)	Molecular weight	86	kg/kmol

6

| Concentration	50	wt.%	Viscosity	0.0038	kg/(m.s)
Specific heat	2.151	kJ/(kg.K)			

6. Results and discussion

First, verification has been carried out to validate the numerical modeling; then, the modeling results are presented.

6.1. Comparison with measured values – Model validation

6.1.1 First validation

Sim et al. [16] researched the boiling of the LiBr/H_2O solution with a concentration of 50 wt.% for bare, notched fin, and low fin tubes. As shown in Figure 3, they used a device where the LiBr/H_2O solution 40 ml covered a tube with a length of 1000 mm. This device included three test sections and a water circulation system. The test section was made of stainless steel with 200 mm internal diameter, 1000 mm length, and 15 mm width. The bare tube was installed in the center of the test section using the flange and O-rings. The water circulation system included a constant temperature hot-water tank, a pump (Wilo, PM-750SI), a mass flow meter, and a manual control valve.
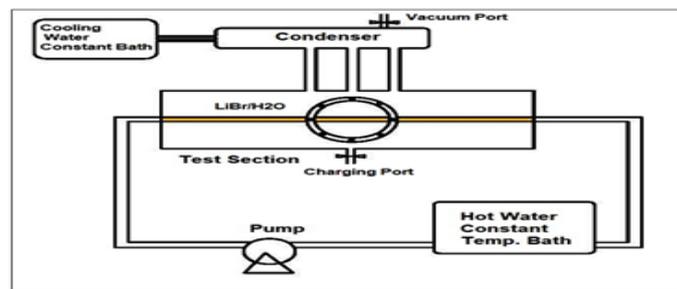
Figure 3. The test ring for pool boiling study

The heat flux of the test tube was controlled with the water temperature of the constant temperature hot-water tank, and the concentration of the LiBr/H_2O solution was measured using a float-type densitometer. They first experimented with pure water at an atmospheric pressure to verify their results and obtained the boiling heat transfer coefficient at different heat fluxes. In the present study, to verify the simulation results, a two-dimensional axisymmetric numerical grid is considered, and the obtained boiling heat transfer coefficient at different heat fluxes is compared with the experimental results. As shown in Table 5, the maximum result difference is 3.3%. The error can also be due to various factors, such as neglecting the contact angle for wall adhesion and considering constant thermophysical properties of the LiBr/H_2O solution.

Table 5. Validation of the boiling heat transfer coefficient of bare tube (Pure water, 101 kPa)

Heat flux (W/m^2)	Sim et al. [16,18]	Present study	Error%
	$h_{Exp.}$ (W/m^2.K)	$h_{Num.}$ (W/m^2.K)	
15020	2368	2400	1.33
30132	3572	3454	3.3
39920	4386	4422	0.82

The experimental results also showed that the extended surface copper tubes have a higher boiling heat transfer coefficient than the bare tube. The results of the present computer simulation

research and the experimental study are the same. Numerical and measured results show that the heat transfer coefficient increases by adding the fin to the bare tube.

6.1.2 Second validation

Varma et al. [31] performed an experimental test to calculate the convective heat transfer coefficient for lithium bromide solution with concentration of 30 wt.% and test ring with a bare copper tube of 14.05 mm diameter and 240 mm length at heat fluxes between 30 to 100 kW/m^2 and a pressure of 6.67 kPa. The second validation was carried out for lithium bromide solution with a concentration of 30 wt.% and other similar specifications of the Varma et al. experimental test, and the heat transfer coefficient of the solution was calculated and plotted in Figure 4.As it is evident, the numerical and experimental results have a good agreement, and the maximum difference between them is less than 18%. The most important reason for this value is because of the constant lithium bromide solution properties.
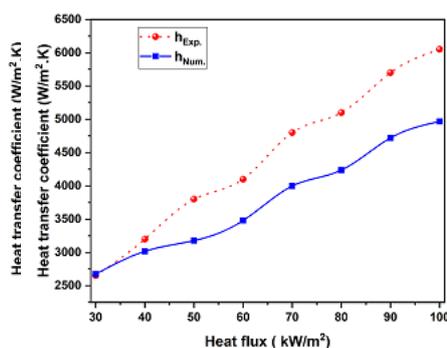
Figure 4. The heat transfer coefficient characteristics of LiBr/H$_2$O with heat flux

6.2. Grid-independence study

The grid independence analysis is a crucial factor in the numerical study. The computation solution needs to be mesh independent for obtaining reliable results. The grid independence study has been conducted on analyzing the boiling heat transfer coefficient for a bare tube in the water at atmospheric pressure. As shown in Table 6, the effect of changing the number of grids of the computational domain is examined on the boiling heat transfer coefficient. The grid in which the obtained value has the smallest difference with experimental value is considered as the study grid. A similar strategy has been carried out for other tube types.

Table 6. Grid independence study results for the bare tube

	Number of cells	h$_{Num.}$ (W/m^2.K)	Error%
Coarse grid	6778	5616	36
Medium grid	29028	3454	3.3
Fine grid	56000	3936	9.2

### 6.3. Pool boiling effect on the generator of absorption chiller

No numerical simulation has been performed despite the experimental research on the benefits of using extended surface tubes in the absorption chiller generator. The numerical simulation results of the LiBr/H$_2$O solution boiling for three different surface types along with nucleation sites, bubble formation time, and bubble separation period are presented. The ANSYS Fluent's output data was first imported to the Tecplot, and then the contours were made. Figure 5 shows the contour of the liquid phase at a heat flux of 400 kW/m^2 for LiBr/H$_2$O solution with a concentration of 50 wt.% and a

pressure of 7 kPa at different times for a bare copper tube, notched fin copper tube, and low fin copper tube, respectively. The red and blue regions indicate a high-density phase (continuum of liquid) and low-density (discrete or vapor phase), respectively. It can be observed that, for the bare tube, the vapor phase is formed at the 30 seconds after model initialization, but for the notched fin tube, it takes 10
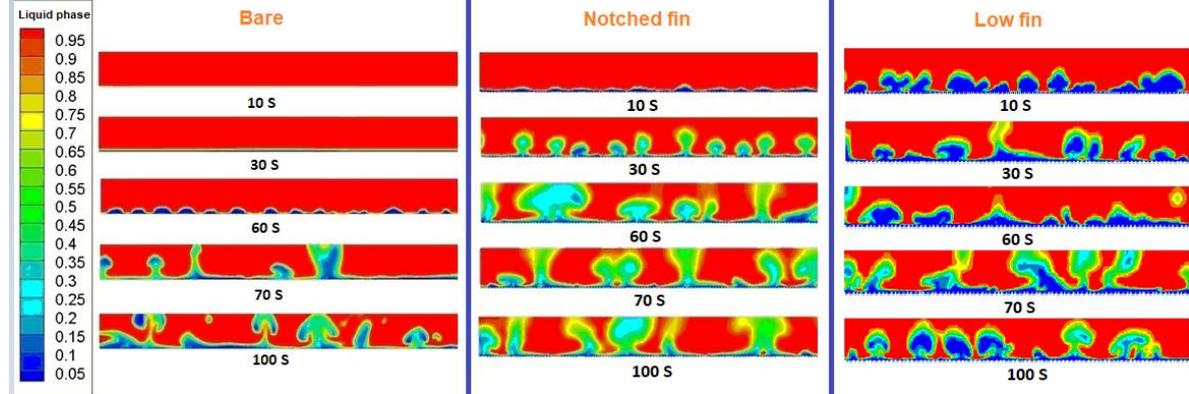
Figure 5. The contour of the liquid phase. a) Bare copper tube, b) Notched fin copper tube, c) Low fin copper tube

The vapor bubbles leave the surface of the bare tube after 70 seconds, while for the notched fin tube, the bubbles leave after 30 seconds. In other words, when the vapor bubbles created on the notched fin-tube and left the surface, at the same time, the bubbles are created on the surface of the bare tube. As shown in Figure 5, after a definite period, the interaction between the bubbles gets more durable, and the small bubbles create large bubbles. In this case, the shape of the bubbles is no longer regular, and because of more fluctuation of the flow, the liquid-vapor interface is also irregular. As can be seen in the results of Figure 5, for low fin tube, phase change happens quickly, and the bubble departs the tube surface in less time rather than other tubes mentioned above.
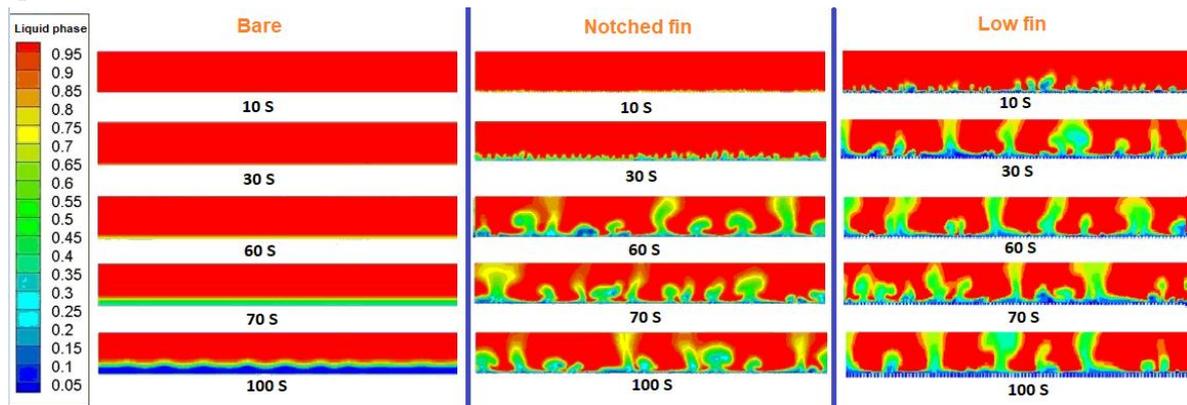
Figure 6. The contour of the liquid phase. a) Bare copper tube. b) Notched fin copper tube. c) Low fin copper tube

Figure 6 shows the liquid phase for bare copper tube, notched fin copper tube, and low fin copper tube at a heat flux of 100 kW/m^2. By comparing these figures, it can be observed that the use of a low fin tube will lead to an increase in the nonhomogeneous nucleation rate due to the creation of the porous structure. Since the free energy is reduced, the creation of bubbles and the capsulated gases in the surface cavities require lower superheat temperature for nucleation. Since in the present study, lithium bromide solution has been considered. As the surface temperature rises, the solution boils on the surface, causing the bubbles to form in some cavities and begin to nucleate, the number of which is a function of the thermal flux that is transferred to the fluid through the surface. The bubbles continue to

appear due to inertia and heat dissipation parameters. The inertia results from existing momentum to move the liquid, and the heat dissipation results from the heat diffusion of the surrounding superheated liquid to the contact surface until the buoyancy force overcomes the surface tension. Furthermore, the bubble leaves the surface. The separation of water bubbles increases the concentration of lithium bromide solution, which decreases the thermal conductivity and its specific heat and increases its density and surface tension, which ultimately decreases the solution's thermal diffusivity. These factors, in constant heat flux, decrease the bubble aggregation rate, forming larger bubbles over time. Three different cases were observed for these nucleation sites: the active cavities nucleate, the static, and inactive cavities do not nucleate. However, they contain the vapor, which may nucleate, disappeared, or filled cavities that lack vapor and only nucleate when the superheat temperature reaches the corresponding temperature of the homogenous nucleation. Using the low fin and notched fin in the generator of absorption chiller leads to create a porous structure as well as a reduction in the wettability of the tube's surface. The surface wettability of the generator's tubes is an essential parameter in the nonhomogeneous boiling, causing the boiling of the $LiBr/H_2O$ solution to start earlier and increasing the heat transfer coefficient. On the other hand, using extended surface tubes before the critical heat flux results in accelerating free convection and nucleate pool boiling steps that cause an increase in the boiling heat transfer coefficient. Nevertheless, after the critical heat flux, due to the complete coating of the tube with a vapor layer that acts as an insulator, it reduces the boiling heat transfer coefficient. Typical absorption chillers with bare tubes in the generator were compared to other types of chillers, which same as vapor compression chillers, require a longer time to produce nominal cooling capacity. Therefore, using low fin tubes in the generator reduces the required thermal energy and time for boiling the $LiBr/H_2O$ solution. Consequently, it leads to a significant discount in adequate time for reaching the chiller's nominal cooling capacity.

7. Conclusion

In this study, the transient two-dimensional numerical modeling of $LiBr/H_2O$ solution pool boiling in the generator of the absorption chiller was carried out by using the Eulerian-Eulerian two-phase approach, extended RPI boiling model, and RNG K-ε turbulence model. This study was conducted to investigate the effect of using extended surface tubes in order to improve the pool boiling phenomena in the generator of absorption chillers. The highlights of the present numerical study are presented as follows:

- ❖ The effects of adding fin on bubble dynamics of $LiBr/H_2O$ solution:
  - • Increasing the bubble growth, bubble merging, and bubble departure rate. These are more evident in the low-fin tube than the notched fin and bare tubes.
  - • Adding low-fin to bare tube increases active nucleation sites which their active function in producing, growing, and departure bubbles occur at certain times, and sometimes show periodic function and become inactive.
  - • As the time of study increases due to more temperature difference between the hot surface and saturation temperature of the $LiBr/H_2O$ solution, the bubble mushroom shape is more likely formed in the low fin and notched fin tubes than the bare tube.
- ❖ The effect of adding fins to improve wettability of $LiBr/H_2O$ solution:
  - • In the case of low fin tube, the static contact angle is higher than in other tubes, resulting in less wettability and less boiling time than notched fin and bare tubes.
- ❖ The effect of adding fin to improve pool boiling of $LiBr/H_2O$ solution:

- Using finned tube same as low fin or notched fin for heat flux lower than the critical heat flux can lead to a faster pool boiling process and an increase in the boiling heat transfer coefficient, which indicates a qualitative improvement in pool boiling.

The results of the present study could help manufacturers and researchers of absorption chillers in selecting a suitable tube type for better performance of chiller with lower cost in comparison to using experimental methods.

Acknowledgement

Nomenclature		Subscripts	
A, C_P	Area (m^2), Specific heat (kJ/kg.K)	b, C	Based, Convection
D, f	Diameter (m), Frequency (Hz)	Crit, E	Critical, Evaporation
h	Convection heat transfer (W/m^2.K)	l, v	Liquid, vapor phase
K, N	Thermal conductivity (W/m.K), Nucleation site	V, Q, w	Vapor, Quenching, Wall
Q, q	Heat transfer (kW), Heat transfer flux (kW/m^2)	**Greek symbols**	
T	Temperature (K)	α, ρ	Phase volume fraction, Density (kg/m^3)

References

[1] Labus, J. M., Bruno, C. J., Coronas, A. Review on absorption technology with emphasis on small capacity absorption machines, *Thermal Science* ,(2013), 17, pp.739-762

[2] Misyura, S.Y. Heat transfer and evaporation of salt solution on a horizontal heating wall, *Thermal Science* ,(2020), 24, pp.2171-2179

[3] Kumar, B., Selvarasan, I., Annadurai, G., Ramalingam, S. Thermodynamic analysis of a single effect lithium bromide water absorption system using waste heat in sugar industry, *Thermal Science* ,(2018), 22, pp.507-517

[4] Zhou, J., Li, S., Li, S. Simulation analysis of performance optimization of gas-driven ammonia water absorption heat pump, *Thermal Science* ,(2020), 00, pp.63-63

[5] Luo, C., Zhao, J., Ma, W. Heat-transfer characteristics of ammonia-water falling film generation outside a vertical tube, *Thermal Science* ,(2017), 21, pp.1251-1259

[6] Ben, H., Mohamed, B., Belghaieb, J., Hajji, N. Numerical study of heat and mass transfer enhancement for bubble absorption process of ammonia-water mixture without and with nanofluids, *Thermal Science* ,(2018), 22, pp.3107-3120

[7] Kunkelmann, C., and Stephan, P., CFD simulation of boiling flow using the volume of fluid method within Open Foam, *Numerical Heat Transfer*,(2009), 56, pp.1-15

[8] Kharangate, CR., Mudawar, I., Review of computational studies on boiling and condensation, *International Journal of Heat and Mass Transfer*,(2017),108, pp.1-33

[9] Mohaghegh, M. R., Rahimi, A. B. Modeling of nucleate boiling heat transfer of a stagnation-point flow impinging on a hot surface, *Thermal Science* ,(2019), 23, pp.695-706

[10] Arshi, B.P.S., Sudharsan, N.M.. Experimental heat and mass transfer studies on horizontal falling film absorber using water-lithium bromide, *Thermal Science*, (2020), 24, pp.1923-1934

[11] Jakubowska, B., Mikielewicz, D. An improved method for flow boiling heat transfer with account of the reduced pressure effect, *Thermal Science*, (2019), 23, pp.1261-1272

[12] Jakubowska, B., Mikielewicz, D. An improved method for flow boiling heat transfer with account of the reduced pressure effect, *Thermal Science*, (2019), 23, pp.1261-1272

[13] Misyura, S.Y. Non-isothermal desorption and nucleate boiling in a water-salt droplet LiBr, Thermal Science, (2018), 22, pp.295-300

[14] Nakoryakov, V.E., Misyura, S.Y., Elistratov, S.L. Nonisothermal desorption of droplets of complex compositions, *Thermal Science*, (2012), 16, pp.997-1004

[15] Zarzycki, R., Panowski, M. Increase of thermal efficiency of cogeneration plant by waste heat utilisation with absorption heat pump, *Thermal Science*, (2019), 23, pp.1101-1112

[16] Sim, Y-S, Kim, N-H.,Pool boiling performance of notched tubes in lithium bromide solution,*International Journal of Air-Conditioning and Refrigeration*,(2015), 23,pp.1-11

[17] Lee, JH., Kim, DH., Kim, SM., Kim, MS., Kim, IG., Woo, SM., Heat transfer characteristics of a falling film generator for various configurations of heating tubes in an absorption chiller, *Applied Thermal Engineering*,(2018), pp.1-10

[18] Sim, Y-S., Kim, N-H., Pool boiling performance of lithium bromide solution on enhanced tubes, *Journal of Mechanical Science and Technology*, (2015), 29, pp.1-9

[19] ANSYS FLUENT. 2019, Available from: www.ansys.com

[20] Li, H., A Vasquez, S., Punekar, H., Muralikrishnan, R., Prediction of boiling and critical heat flux using an Eulerian multiphase boiling model. *Proceedings of the ASME International Mechanical Engineering Congress & Exposition IMECE*, (2011), pp.25-35

[21] Nguyen, T. T, Duong, H. N, Tran, V. T., Kikura, H., A CFD modeling of subcooled pool boiling,*International Conference on Advances in Computational Mechanics*, (2017), pp. 741-758

[22] Ishii, M., Kim, S., Uhle, J., Interfacial area transport equation: model development and benchmark experiments, *International Journal of Heat and Mass Transfer*, (2002), pp. 3111-3123

[23] Tomiyama, A., Celata, GP., Hosokawa, S., Yoshida, S., Terminal velocity of single bubbles in surface tension force dominant regime, *International Journal of Multiphase Flow*,(2002)

[24] Antal, SP., Jr, RTL., Flaherty, JE., Analysis of phase distribution in fully developed linear bubbly two-phase flow,*Internationa Journal of Multiphase Flow*,(1991)

[25] Bertodano, MLd., RTLahey, JR., OCJone, S., Turbulent bubbly two-phase flow data in a triangular duct, *Nuclear Engineering and Design*, (1994), pp.20-29

[26] Troshko, A., Hassan, YA., A two-equation turbulence model of turbulent bubbly flow, *International Journal of Multiphase Flow*, (2001), pp.23-35

[27] Ranz, WE., Marshall, WR., Evaporation from drops Chemical engineering progress, (1996); pp.6

[28] Tolubinsky, V. I., Kostanchuk, D. M.,Vapor bubbles growth rate and heat transfer intensity at subcooled water boiling,*In Proceedings of the 4th International Heat Transfer Conference*, (1970)

[29] COLE, R., Bubble frequencies and departure volumes at sub atmospheric pressures. *AlChE Journal*, (1967); pp.1-5

[30] Lemmert, M., Chawla, J. M., Influence of flow velocity on surface boiling heat transfer coefficient, *In Heat Transfer in Boiling, E. Hahne and U. Grigull, Eds.*, (1977), pp. 237–247

[31] Varma, H.K., Mehrotra, R.K., Agrawal, K.N., Singh, S., Heat transfer during pool boiling of LiBr-water solutions at sub atmospheric pressures, *International Communications in Heat and Mass Transfer*, (1994), pp. 10-20